Border-Collision Bifurcations in Automatic Control Systems with Two-Side Sinusoidal Unipolar Reversible Pulse-Width Modulation

A.I. Andriyanov

Department of Electronics, Radioelectronic and Electrotechnical Systems, Bryansk State Technical University, Bryansk, Russia
E-mail: mail@ahaos.ru

Received: 20.10.2015

Abstract. This paper considers nonlinear dynamics of automatic control system based on two-side sinusoidal unipolar reversible modulation. Mathematical simulation of the considered system is carried out. The first bifurcation borders in two-parameter state space has been analyzed, that is relevant to the practical side. The paper demonstrates, that in the considered system the first bifurcation borders are critical, as they are related to hard bifurcations. A bifurcation, which corresponds to the variation of the widely-known border-collision bifurcation, was detected at large control signal values. Being characterized by its unique features this bifurcation variation is of great theoretical interest.

Keywords: automatic control system, sinusoidal pulse-width modulation, power inverter, bifurcation, nonlinear dynamics

INTRODUCTION

Single-phase sinusoidal pulse-width modulation inverters are rather widely used owing to their capability to provide high quality AC output voltage and reasonable weight and size. Their common applications are computer uninterruptable power supply units, AC-motor variable speed control, induction heats, etc. [1].

Sinusoidal pulse-width modulation inverters have significant differences in principle of output voltage formation as compared to DC/DC converters [1]. In particular, the systems under analysis are characterized by additional low-frequency periodic action (sinusoidal control signal), which brings about specific characteristics of the nonlinear dynamics of such systems. Currently a small number of works [2] is devoted to the study of bifurcations in systems with sinusoidal modulation, with works devoted to two-side unipolar reversible modulation (URM) missing, which makes this study topical.

CONTROL SYSTEM DESCRIPTION

Equivalent circuit of the closed-loop control system based on two-side unipolar reversible modulation is shown in Fig. 1. The symbols in Fig. 1 correspond to the following: U_{in} – input voltage, L – inductor inductance, C – capacitor capacity, R_L – load resistance, FA – feedback

© Andriyanov, A.I., 2016

amplifier with gain value K_{fb}, *CON* – controller, *MC* – master clock, *RMP*1, *RMP*2 – ramp generators, *CM*1, *CM*2 – comparators, *XOR*1, *XOR*2 – XOR-gates, *VT*1–*VT*4 – power switches, *VD*1–*VD*4 – power diodes, *K*1, *K*2 – bi-directional switches, *TV* – power transformer, U_{ref} – sinusoidal reference signal, U_{con} – control signal, U_{err} – error signal, U_{rm1}, U_{rm2} – ramp generators output signals, U_{cm1}, U_{cm2} – comparators output signals, U_{mc} – master clock output signal.

The specialty of the control system shown in Fig. 1 is two sweep generators, producing respectively rising ramp and falling ramp signals. It also includes two pulse-width modulators, each controlling the corresponding bridge leg composed of two power transistors [3]. When control signal is modified, control pulse of the left bridge leg shifts to the right by the phase angle α, meanwhile control pulse of the right bridge leg shifts to the left by the phase β, where α=β. The power circuit, which is a part of the described control system, is known as a phase-shifted URM-inverter [3].

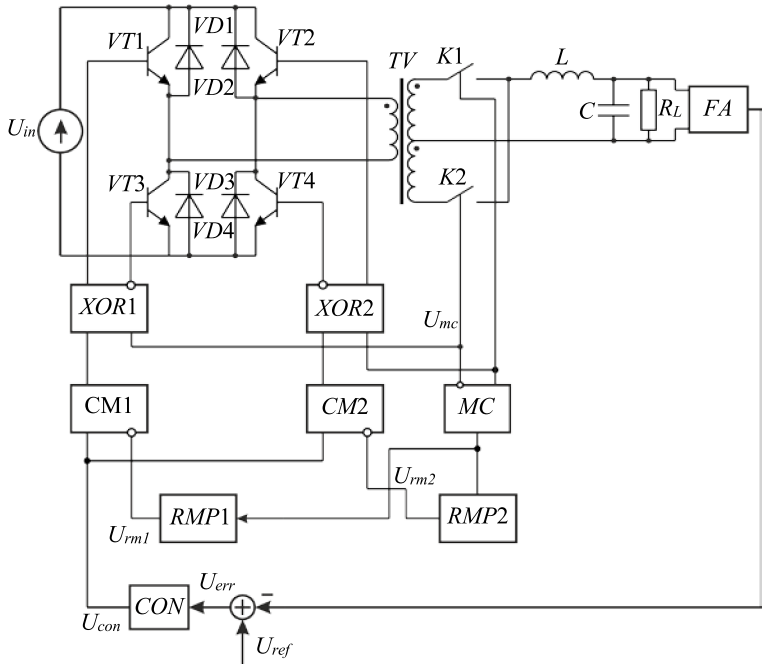

Figure 1. Functional block diagram of closed automatic control system based on URM

Signal waveforms on a modulation period of the system considered are shown in Fig. 2. The symbols in Fig. 2 correspond to the following: z_{ki} – i-th moment of switching in relative time.

The moment of switching in relative time is calculated as:

$$z_{ki} = \frac{t_{ki} - (k-1)T}{T},$$

where t_{ki} – the moment of switching in absolute time, k – the modulation period number, T – the modulation period duration.

Waveform analysis demonstrates that the modulation period can be divided into three intervals of system constancy:

1) interval 1: $0<z<z_{k1}$. Transistors *VT*1, *VT*2 or *VT*3, *VT*4 and bi-directional switch *K*1 or *K*2 are in ON-state. Zero voltage is applied to the power filter input: $U_{inf}=0$;

2) interval 2: $z_{k1}<z<z_{k2}$. Transistors *VT*1, *VT*4 or *VT*2, *VT*3 and bi-directional switch K1 or K2 are in ON-state. In this case voltage across the power filter input (U_{inf}) is respectively positive or negative (Fig. 2);

3) interval 2: $z_{k2}<z<1$. This interval is similar to interval 1.

The automatic control system dynamics on each constancy interval is presented by the corresponding linear differential equation system. The subdivision smooth curves of different intervals are interconnected by fitting procedure. The mathematical model of the system described is given in [4].

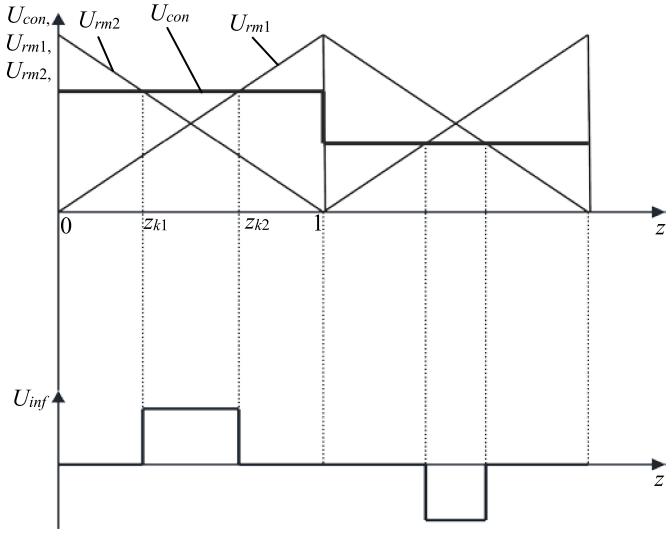

Figure 2. Signal waveforms on a modulation period of the full bridge phase-shifted URM power inverter

The set of linear differential equations that describe the system dynamics on every interval of power circuit structure constancy can be presented in matrix form as:

$$\frac{d\mathbf{X}}{dt} = \mathbf{A}_i\mathbf{X} + \mathbf{B}_i, \tag{1}$$

where $\mathbf{A}_i$ – matrix of constant factors on the i-th interval of power circuit structure constancy, $\mathbf{B}_i$ – vector of forcings on the i-th interval of power circuit structure constancy, $i = 1, 2$, $\mathbf{A}_1 = \mathbf{A}_2 = \mathbf{A}_3 = \begin{bmatrix} -\frac{R}{L} & -\frac{1}{L} \\ \frac{1}{C} & -\frac{1}{CR_L} \end{bmatrix}$, $\mathbf{B}_2 = \begin{bmatrix} U_{in}/L \\ 0 \end{bmatrix}$, $\mathbf{B}_1 = \mathbf{B}_3 = \begin{bmatrix} 0 \\ 0 \end{bmatrix}$, $\mathbf{X}=[x_1, x_2]=[i_L, u_C]$ – vector of state variables, i_L – inductor current, u_c – capacitor voltage.

The integration results (1) are presented in analytical form with transition from one interval to another implemented by curve fitting technique.

Hereafter the author demonstrates that the system behavior on the k-th modulation period can be described by the function of stroboscopic maps as follows:

$$\mathbf{X}_k = \Psi(\mathbf{X}_{k-1}) = e^{\mathbf{A}a}\mathbf{X}_{k-1} + (e^{\mathbf{A}a} - e^{\mathbf{A}(1-z_k)a})\mathbf{A}^{-1}\mathbf{B}, \tag{2}$$

where $\mathbf{X}_{k-1}$ – vector of state variables at the beginning of the k-th modulation period.

In the case of sinusoidal URM control signal period contains integral number of modulation periods q, where q is quantization ratio. Therewith the function of stroboscopic maps for the system with sinusoidal URM can be defined as follows:

$$\mathbf{X}_p = \Psi^{(q)}(\mathbf{X}_{p-1}) \equiv \underbrace{\Psi \circ \Psi \circ \Psi \circ \Psi \circ \ldots \circ \Psi}_{q \text{ times}}, \tag{3}$$

where p – stroboscopic maps iteration number.

Switching moments z_{k1} and z_{k2} on the k-th modulation period can calculated from the equation of switching varifold $\xi(\mathbf{X},z_{k1})=0$, where switching function is given by [2]:

$$\xi(\mathbf{X}, z_k) = \alpha\left(U_{ref}(k) - \beta u_c(k)\right) - U_{rgm} z_k,$$

where $u_c(k)$ – capacitor voltage at the beginning of the k-th modulation period, U_{rgm} – ramp signal amplitude, $U_{ref}(k)= U_{rgm}/2+U_{rm}\sin(\omega_c(k-1)T)$, U_{rm} – reference signal amplitude.

As can be seen in Fig. 2 on account of modulation period symmetry $z_{k2}=1 - z_{k1}$.

MATHEMATICAL SIMULATION

Mathematical simulation of inverter operation with two-side unipolar reversible modulation was carried out as part of the study. The following set of parameters was selected as part of the calculations: U_{in}=50 V, quantization ratio q=10, R_L=45 Ohm, quantization frequency f_{qu}=10 kHz, R=1 Ohm, L=4 mH, C=3.5 μF, ramp signal U_{rmpm}=±10 V, coefficient of proportional regulator K=50, feedback gain K_{fb}=0.015.

Fig. 3a (U_{rm} – reference signal amplitude) shows a dynamical modes map with marked areas of existence of different modes in the space of two parameters: reference signal amplitude of voltage output U_{rm} and input voltage U_{in}.

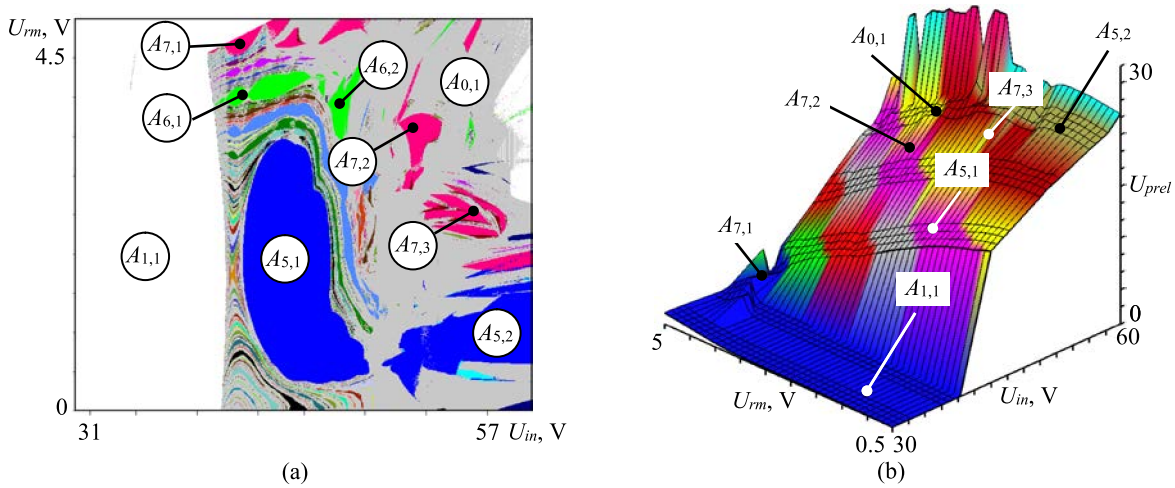

Figure 3. Two-parameter diagrams: dynamical modes map (a); relative RMS-value of output voltage parasitic harmonics (b)

Fig. 4 shows the bifurcation diagram and monodromy matrix large multiplier module diagram of mode $R^s_{1,1}$ (i_L – inductor current). This mode corresponds to the area $A_{1,1}$ in Fig. 3a.

The map has areas of existence of different dynamical modes marked with symbols $A_{i,j}$ (i is an m-cycle peculiar to this area, therewith, when i=0, the area corresponds to a region of existence of chaotic oscillations; j is a number of the area on the dynamical modes map). Fig. 3b shows a two-parameter diagram of relative RMS-value of output voltage parasitic harmonics (U_{prel}), that can be calculated as:

$$U_{prel} = \frac{U_p}{U_{1max}},$$

where U_p – RMS-value of output voltage parasitic harmonics, U_{1max} – maximum RMS-value of the wanted harmonic in the area of the design mode.

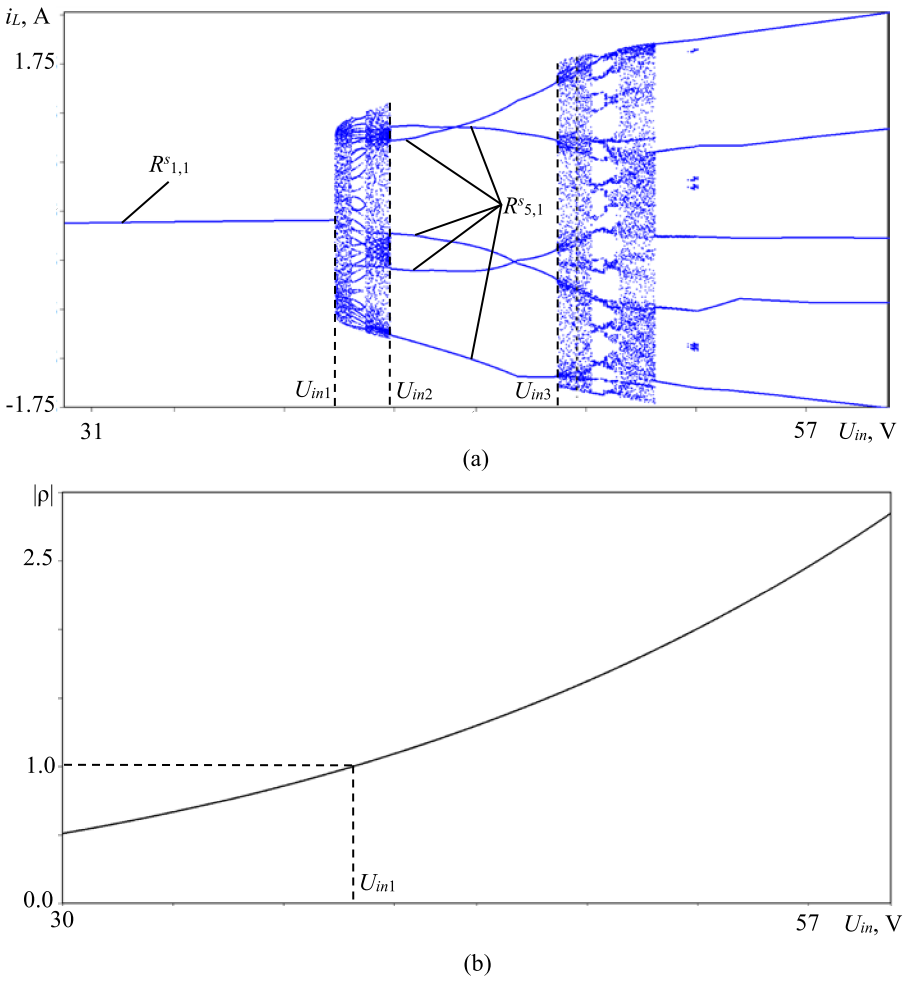

Figure 4. Diagrams at U_{rm}=1 V: bifurcation diagram (a); large multiplier module diagram (b)

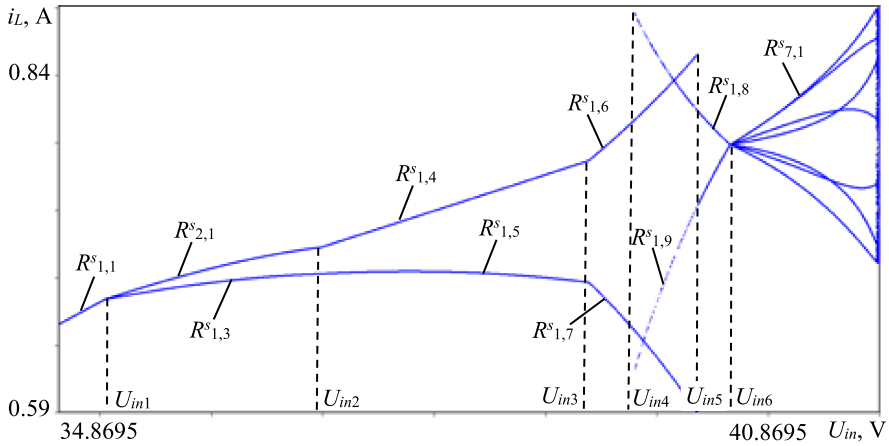

Figure 5. Bifurcation diagram at U_{rm}=4.75 V

The analysis of these diagrams shows that the first bifurcation point (U_{in1}=39.846 V) is due to Neumark-Sacker subcritical bifurcation (complex large multiplier module at the bifurcation point intersects the unity). This bifurcation is obscure and determines the segment AB of the first bifurcation border.

Fig. 5 shows a bifurcation diagram with U_{rm} =4.75 V, corresponding to dynamical modes map (Fig. 3a).

The first bifurcation point U_{in1}=34.917 V is associated with a border-collision bifurcation of pitch-fork type (Fig. 6, where u_c – capacitor voltage), with two stable 1-cycles $R^s_{1.2}$ and $R^s_{1.3}$ following the bifurcation, and 1-cycle $R^s_{1.1}$ transition to unstable 1-cycle $R^u_{1,5}$ with another symbolic characteristics. The definition of a symbolic characteristic is given in [5].

The bifurcation point U_{in2}=36.848 V (Fig. 5) features a bifurcation of a simple change of the solution type for a pair of 1-cycles. The symbolic characteristic of the first 1-cycle is changed during transition from $R^s_{1,2}$ to $R^s_{1,4}$, and the symbolic characteristic of the second 1-cycle is changed during transition from $R^s_{1,3}$ to $R^s_{1,5}$.

The bifurcation point U_{in3}=39.25 V (Fig. 5) features another change of symbolic characteristics for the pair of 1-cycles. The symbolic characteristic of the one 1-cycle is changed during transition from $R^s_{1,4}$ to $R^s_{1,6}$, and the symbolic characteristic of the other 1-cycle is changed during transition from $R^s_{1,5}$ to $R^s_{1,7}$.

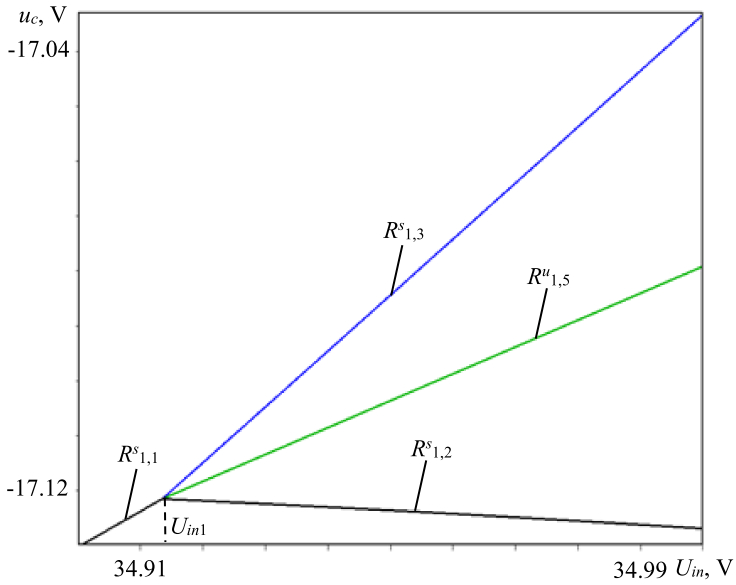

Figure 6. Detailization 1 of the bifurcation diagram at U_{rm}=4.75 V

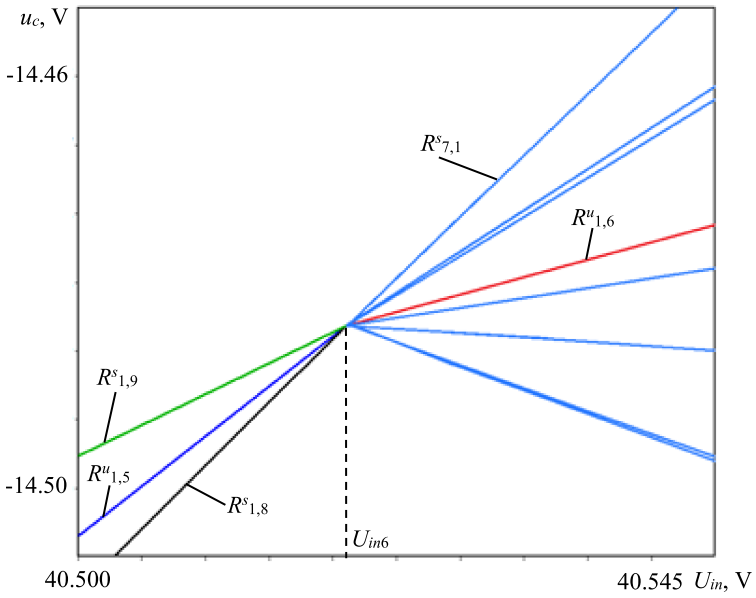

Figure 7. Detailization 2 of bifurcation diagram at U_{rm}=4.75 V

The bifurcation point U_{in4}=39.656 V features a pair of saddle-node border-collision bifurcations. The bifurcation point U_{in4} features the merge of two pairs of 1-cycles with different symbolic characteristics, which corresponds to saddle-node border-collision bifurcations.

A specific bifurcation occurs at the point U_{in6}=40.521 V (it corresponds to BC segment of the first bifurcation border (Fig. 3a)). In this case, the merge of two stable 1-cycles $R^s_{1,8}$ and $R^s_{1,9}$ and an unstable $R^u_{1,5}$ with different symbolic characteristics takes place, followed by the subsequent soft emergence of a stable 7-cycle $R^s_{7,1}$ together with an unstable 1-cycle $R^u_{1,6}$ (Fig. 7). This bifurcation is a kind of border-collision bifurcation. A bifurcation with similar principle is described in [6], but in this case, the bifurcation involves the cycles with the same periodicity equal to 1, thus bearing evidence of the novelty of the observed phenomenon.

CONCLUSION

The bifurcation analysis conducted shows specific behavior of the system with variation of its parameters. A characteristic feature of automatic control pulse-width modulation systems is the presence of a great variety of border-collision bifurcations. It imposes specific requirements to the design mode of SPWM systems. In particular, the design mode of such systems means 1-cycle [4, 5], where all the duty factors on the period of sinusoidal reference voltage must be less than unity and greater than zero. The findings will further allow to create control algorithms for nonlinear dynamics of SPWM systems.

The reported study was supported by RFBR, research project № 14-08-31126 “mol_a”.

REFERENCES

1. B. Ismail, S.T. Mieee, A.R. Mohd, M.I. Saad and C.M. Hadzer, “Development of a Single Phase SPWM Microcontroller-Based Inverter,” in First International Power and Energy. Conference Pecon 2006 November 28-29, Putrajaya, and Malasia, pp. 437–440, 2006.
2. Zh.T. Zhusubaliyev, E. Mosekilde, A.I. Andriyanov and V.V. Shein, “Phase Synchronized Quasiperiodicity in Power Electronic Inverter Systems,” Physica D: Nonlinear Phenomena, vol. 268, pp.14–24, 2014.
3. A.V. Kobzev, G.Ya. Michal’chenko and N.M. Muzhitchenko, Modulating Power Supplies of Radioelectronic Devices, Tomsk: U.S.S.R.: Radio i Svyaz, 1990.
4. A.I. Andriyanov and G.Ya. Mikhalchenko, “Problems of mathematical modeling of the closed-loop systems of automatic control on the basis of unipolar reversible modulation,” Mekhatronika, avtomatizaciya, upravlenie, No. 1, pp. 11–19, 2005.
5. Zh.T. Zhusubaliyev and Yu. V. Kolokolov, Bifurcations and chaos in relay and pulse-width automatic control systems, Moscow: Mashinostroenie-1, 2001.
6. Zh. T. Zhusubaliev, E.A. Soukhoterin and E. Mosekilde, “Border-collision bifurcations and chaotic oscillations in a piecewise-smooth dynamical system,” Int. J. Bifurcation Chaos, vol. 11, No. 12, pp. 2977–3001, 2001.